Modeling of Void Swelling in Irradiated Steels

B. Glasgow and W.G. Wolfer

June 1984

UWFDM-586

Presented at the 12th Intern. Symposium on the Effects of Radiation on Materials, Williamsburg, VA, June 18-20, l984.

FUSION TECHNOLOGY INSTITUTE

UNIVERSITY OF WISCONSIN

MADISON WISCONSIN

"LEGAL NOTICE"

"This work was prepared by the University of Wisconsin as an account of work sponsored by the Electric Power Research Institute, Inc. ("EPRI"). Neither EPRI, members of EPRI, the University of Wisconsin, nor any person acting on behalf of either:

"a. Makes any warranty or representation, express or implied, with respect to the accuracy, completeness, or usefulness of the information contained in this report, or that the use of any information, apparatus, method, or process disclosed in this report may not infringe privately owned rights; or

"b. Assumes any liabilities with respect to the use of, or for damages resulting from the use of, any information, apparatus, method or process disclosed in this report."

DISCLAIMER

This report was prepared as an account of work sponsored by an agency of the United States Government. Neither the United States Government, nor any agency thereof, nor any of their employees, makes any warranty, express or implied, or assumes any legal liability or responsibility for the accuracy, completeness, or usefulness of any information, apparatus, product, or process disclosed, or represents that its use would not infringe privately owned rights. Reference herein to any specific commercial product, process, or service by trade name, trademark, manufacturer, or otherwise, does not necessarily constitute or imply its endorsement, recommendation, or favoring by the United States Government or any agency thereof. The views and opinions of authors expressed herein do not necessarily state or reflect those of the United States Government or any agency thereof.

Modeling of Void Swelling in Irradiated Steels

B. Glasgow and W.G. Wolfer

Fusion Technology Institute
University of Wisconsin
1500 Engineering Drive
Madison, WI 53706

http://fti.neep.wisc.edu

June 1984

UWFDM-586

Presented at the 12th Intern. Symposium on the Effects of Radiation on Materials, Williamsburg, VA, June 18-20, l984.

B. B. Glasgow and W. G. Wolfer*

MODELING OF VOID SWELLING IN IRRADIATED STEELS

REFERENCE: Glasgow, B. B. and Wolfer, W. G., "Modeling of Void Swelling in Irradiated Steels", Effects of Radiation on Material: Twelfth Conference, American Society for Testing Materials, 1984.

ABSTRACT: The theory of void swelling in irradiated steels has been critically re-examined and a model has been developed from first principles for such fundamental parameters as the bias factors for dislocations and voids, relaxation volumes for interstitials and vacancies, and migration and formation energies for interstitials and vacancies. Four types of growth mechanisms are modeled: self-interstitial emission, loop punching, thermal vacancy exchange, and bias driven growth. The net bias of the system is allowed to change continuously with the evolving microstructure. Combining these growth mechanisms has resulted in a swelling model capable of reproducing some important features of the observed swelling behavior in austenitic stainless steels. For austenitic stainless steels the model predicts bias driven growth for temperatures between $300°C$ and $600°C$. The long term swelling rate in this temperature range is roughly independent of temperature and helium concentration and is between 0.7 %/dpa and 1.3 %/dpa. For ferrite phase the model predicts bias driven growth for temperatures between $300°C$ and $500°C$. However, for this class of steel the swelling rate is at or below 0.3 %/dpa. For bias driven growth it has been shown that the interstitial and vacancy relaxation volumes ultimately determine the maximum possible swelling rate. It is for this reason the model predicts a much lower swelling rate for ferrite phase than for austenitic stainless steels.

KEY WORDS: radiation effects, void swelling, helium equation of state, dislocation evolution

Introduction

Recent analysis [1] of swelling data for austenitic stainless steels has revealed that the steady state swelling rate is nearly independent of temperature. Furthermore, the

* Graduate student and professor, respectively, Fusion Engineering Program, Nuclear Engineering Department, University of Wisconsin - Madison, Madison, WI 53706

swelling rate appears to approach an ultimate value of about 1 %/dpa independent of the initial microstructure and independent of the alloy composition. These observations are in contradiction with earlier analyses. Accordingly, the physical processes of swelling have been reexamined from first principles and have been refined and a rate theory model of swelling has been developed. Additionally, initial experimental results [2] of the swelling of ferritic steel suggest a much lower swelling rate for this class of steel. However, long term exposure results have not yet been completed. In an effort to predict the steady state swelling behavior of ferritic steels, the rate theory model of swelling is applied to ferrite phase.

The rate theory of swelling is basically concerned with the calculation of the net flux of point defects to the surface of a void or bubble. Knowing the net flux to a cavity surface, the growth rate can be calculated. The major unknowns to be determined in this rate theory are the sink strengths and the bias factors of cavities and dislocations.

As a result of the continuous helium production, other growth mechanisms are also possible and are incorporated in the present model. These gas-driven mechanisms are as follows.

1. Thermal vacancy exchange. Due to differences in the equilibrium vacancy concentrations between the cavity surface and the bulk material, thermally generated vacancies will tend to flow either toward or away from cavity surfaces.
2. Loop punching. Given a sufficiently high pressure and energetically favorable conditions, it has been shown [3] that an interstitial platelet can be punched out from the bubble surface.
3. Self-Interstitial Emission. Given high enough pressure within a bubble, a self-interstitial can be emitted from a bubble surface.

The results of the model presented herein do not accurately match experimentally determined swelling behavior. This is to be expected because of many simplifying assumptions made. For example, the only sinks modeled are cavities and dislocations. The nucleation of cavities is not modeled; rather, a constant number of cavities is assumed with a uniform radius which increases with time. It is assumed that all of

the helium is equally partitioned to the cavities. Even though certain aspects of the physical processes are not modeled, important features of swelling behavior result. These features include a steady state swelling roughly independent of temperature, a significantly lower swelling rate for ferrite phase than for austenitic stainless steels, and an incubation-type period early in life which depends on the helium concentration and pressure. Temperature independent steady state swelling rate and an incubation period have been reported [1] in experimental results; and helium is considered to be a major factor in causing early nucleation of cavities in steels exposed to neutrons.

Helium Equation Of State

Helium produced by (n, α) reactions or injected in metals is essentially insoluble. Therefore, helium has the natural tendency to precipitate and form bubbles. The pressure in the bubbles can become quite large. The experimentally determined equation of state does not cover at the present time the entire range of interest of temperature and pressure. In an effort to predict the pressure in helium bubbles correctly, a theoretical equation of state was developed by Wolfer et al. [4]. A brief explanation of the equation of state is as follows.

Gaseous helium is modeled by perturbation theory [5] to be a system of hard spheres of diameter d which is dependent on temperature and the packing fraction $y = \frac{\pi}{6} d^3 \frac{m}{V}$, where m is the number of helium atoms and V is the volume of a cavity. Then the compressibility factor in the hard sphere approximation is given by the Carnahan and Starling approximation [6]; $z_{hs} = (1+y+y^2-y^3)/(1-y)^3$. Two contributions are added to z_{hs}. First, a quantum correction z_Q is obtained with the interatomic potential of helium and the radial distribution function. Second, to account for the attractive part of the atomic potential, another correction z_A is included. This attractive correction z_A is a function of the width and depth of the potential well. The total compressibility is then given by $z = z_{hs} + z_Q + z_A$. The solid helium equation of state is found by determining the free energy of the lattice atoms as the sum of the ground state potential energy plus the vibrational energy about the lattice equilibrium points. The ground

state pressure p_o has been determined by several researchers [7,8]. Their results are used in the model. To establish the vibrational energy contribution to the pressure, the Debye theory is employed with a temperature dependent Debye temperature. The actual compressibility factor z is then given by either the gaseous or the solid equation of state depending on the density and temperature of the helium.

While the theoretical equation of state described above gives good agreement with available experimental data, it is cumbersome to use. To make the results of the equation of state easier to apply, a simple polynomial fit to the data was obtained for the two regions (gaseous and solid). The fitted equations are presented below.

For low densities, covering the gaseous state, the compressibility factor can be approximated by

$$z = A_g + B_g x + C_g x^2 + D_g x^3, \qquad x \leq 1.7\,T^{0.41} \tag{1}$$

where x is the helium density in (100 moles/cm^3) and

$$\begin{aligned} A_g &= (T/1300)^{\frac{1}{25}} \\ B_g &= 5.83(1/T)^{0.58} \\ C_g &= \frac{\log_{10}(T/800)}{0.69T^{0.65}} \\ D_g &= 8.6(1/T)^{1.44} \quad . \end{aligned}$$

T is the absolute temperature. For the solid fitted equation of state,

$$z = A_s + B_s x + C_s x^2, \qquad x \geq 1.7\,T^{0.41} \tag{2}$$

where

$$\begin{aligned} A_s &= -3.89 + 6.59 \times 10^{-2}T - 1.15 \times 10^{-4}T^2 + 5.46 \times 10^{-8}T^3 \\ B_s &= -0.523 + 4.39 \times 10^{-4}T + 1.77 \times 10^{-6}T^2 - 1.37 \times 10^{-9}T^3 \\ C_s &= 0.101 - 2.91 \times 10^{-4}T + 3.01 \times 10^{-7}T^2 - 1.045 \times 10^{-10}T^3. \end{aligned}$$

Figure 1 gives the comparison for the compressibility according to the theory and the polynomial fit for three different temperatures, 200, 600, and 1000^oK. Within the

ranges of $200 \leq T \leq 1200^o K$ and $0 \leq x \leq 50$ (100 moles/cm^3), the agreement is within 11 %.

Athermal Growth Processes

Two different athermal growth mechanisms are considered in the model: 1) self-interstitial emission and 2) interstitial loop punching. These two mechanisms are activated only at relatively high pressures.

Glasgow and Wolfer [9] concluded that self-interstitial emission is energetically favored over helium interstitial emission, and that the condition required for bubble growth by self-interstitial emission is

$$p\Omega \geq \frac{2\gamma\Omega}{R} + E_i^f + E_i^m + kT \ln \left[\frac{\eta \dot{P}}{4\pi R N D_i^o} \right] . \tag{3}$$

It was found that the overwhelming contribution to the right hand side originates from E_i^f, the interstitial formation energy; and that p must be on the order of 10^{10} Pa for the condition to be satisfied. The other parameters included in the above equation are as follows: Ω is the atomic volume, γ is the cavity surface energy, R is the cavity radius, E_i^m is the interstitial migration energy, k is Boltzmann's constant, T is the temperature, D_i^o is the pre-exponential interstitial diffusion constant, $\dot{P}$ is the helium production rate, η is the ratio of helium atoms to vacancies in a cavity, and N is the cavity number density.

Instead of the emission of one interstitial at a time, it is possible that an entire interstitial platelet may be emitted. Trinkaus [10] and Greenwood et al. [11] have shown that the condition for loop punching is

$$p\Omega \geq \frac{(2\gamma + \mu b)\Omega}{R} \tag{4}$$

when the bubble radius R is less than about $15b$. Here, μ is the bulk modulus and b is the Burgers vector. As can be seen, there is a radial dependence for loop punching, whereas self-interstitial emission is nearly independent of the bubble radius. While

self-interstitial emission is favored over loop punching at small radii, the opposite is true at larger radii.

Athermal processes can be activated only if the above described conditions are satisfied. To determine if either of the two conditions is satisfied, it is assumed that a density of cavities (dependent on temperature) with a uniform radius exists and that all helium atoms are evenly distributed among the cavities. The pressure within the cavities can be found using the equation of state and compared with the two criteria. If one of the two criteria embodied in Equations (3) and (4) is satisfied, the cavity radius is increased incrementally until the pressure drops below the critical values for self-interstitial emission and for loop punching. It has been found that athermal cavity growth is significant only under extremely high helium production or implantation rates as is seen in blistering studies.

Bias Driven Growth And Thermal Vacancy Exchange

According to the rate theory of void growth the swelling rate is given by

$$\frac{d}{dt}\left(\frac{\Delta V}{V}\right) = 4\pi N R Z_v^o D_v \left[\frac{\bar{Z}_i}{\bar{Z}_v} - \frac{Z_i^o}{Z_v^o}\right]\Gamma - D_v(C_v^o - \bar{C}_v) \tag{5}$$

where N and R are the cavity number density and radius, respectively. $4\pi NR$ is known as the void sink strength (S_o). D_v is the vacancy diffusion coefficient, $\bar{Z}_{i,v}$ and $Z_{i,v}^o$ are the average bias factors for interstitials and vacancies and the void bias factors for interstitials and vacancies, respectively. $\bar{C}_v$ is the sink-averaged vacancy concentration and C_v^o is the vacancy concentration in equilibrium with a cavity. Γ is defined as

$$\Gamma = \frac{S}{2\lambda D_v}[\sqrt{\alpha^2 + \beta} - \alpha] \tag{6}$$

where $\lambda = 4\pi R_c/\Omega$, R_c is the recombination radius. $\alpha = 1 + \lambda \bar{C}_v/(S\bar{Z}_i)$, $\beta = 4\lambda D_v P_{pd}/(S^2 \bar{Z}_i \bar{Z}_v)$, P_{pd} is the production rate of point defects. S is the total sink strength, and is composed of the void sink strength (S_o) and the dislocation sink strength (S_d).

The second term in Equation (5) is due to the flow of vacancies to or away from the cavities, depending on the vacancy concentration in local thermodynamic equilibrium with the cavity. This concentration is given by

$$C_v^o = C_v^{eq} \exp\left(\frac{p_o \Omega}{kT}\right) \tag{7}$$

where $p_o = (2\gamma/R - p)$ and C_v^{eq} is the thermal equilibrium vacancy concentration. For over-pressurized bubbles ($p > 2\gamma/R$) there will be a net flow of vacancies to the bubble surface. Because of the temperature dependence of D_v, the second term in the swelling rate equation (5) (annealing term) is not important at temperatures below about 500^oC. However, at temperatures above about 600^oC the annealing term is comparable to or larger than the first term (bias term).

The time evolution of the microstructure plays an important role in the bias term. In particular, the sink strengths (S_o and S_d) and the sink-averaged parameters ($\bar{C}_v$, $\bar{Z}_i$, and $\bar{Z}_v$) change with the microstructure. If only two sink types are present, namely cavities of equal radii and edge dislocations, then

$$\text{bias driven swelling rate} \sim \frac{S_0\, S_d}{(S_d + S_o)^2}\left(\frac{Z_v^o\, Z_i^d - Z_i^o\, Z_v^d}{\bar{Z}_i\, \bar{Z}_v}\right)$$

where $Z_{i,v}^d$ is the dislocation bias factor for interstitials and vacancies. From this expression it can be seen that sink strengths and sink-averaged bias factors are important for bias driven growth. It is also evident that the maximum swelling rate for bias driven growth is attained when the void sink strength equals the dislocation sink strength as pointed out by Harkness and Li [12]. In this case the swelling rate is mainly determined by the bias factors and to a lesser extent by Γ. In turn, the net bias factor is critically dependent on the interstitial and vacancy relaxation volumes as shown by Sniegowski and Wolfer [13].

Dislocation Density Evolution Model

As discussed above, the bias driven swelling rate is a function of sink strengths. Therefore, to model swelling rates, the sink strengths as a function of time should be known.

For the void sink strength the number density is assumed constant, but the radius is changing. For the dislocation sink strength the density of dislocations is evolving through thermal and irradiation processes. As a result of the preferential absorption of interstitials at edge dislocations, dislocations climb and, if pinned by precipitates, increase their line length. Large dislocation loops at higher temperatures make only a small contribution to the dislocation density and are treated approximately as edge dislocation segments. However, experimental observation [14] indicates that at lower temperatures loop density increases and loop size decreases. Therefore, the edge dislocation segment approximation is probably not appropriate at temperatures at or below 300^oC. The present model can therefore not be applied to materials containing a high density of small dislocation loops.

Detailed analysis [15] of the process shows that the rate of increase of the dislocation density is given by

$$B\rho = \rho l \left\{ V_R - V_T \left[1 - \exp\left(\frac{-Hb}{l} \ln \frac{l}{1.8b} \right) \right] \right\}. \tag{8}$$

However, B is set equal to 0 when the right hand side of Equation 8 is negative. In this case, the radiation-induced climb force can no longer overcome the opposing line tension force contained in the argument of the exponential function. In the above equation, l is the average distance between pinning centers, ρ is the dislocation density, b is the Burgers vector,

$$H = \mu\Omega/[2\pi(1-\nu)kT] \tag{9}$$

$$V_T = \frac{\Omega}{b} D_v Z_v^d C_v^{eq} \tag{10}$$

$$V_R = \frac{\Omega}{b} D_v \left[\frac{Z_i^d}{Z_v^d}(1+\varsigma) - \frac{\bar{Z}_i}{\bar{Z}_v} \right] \Gamma. \tag{11}$$

V_R is the radiation induced climb velocity; and V_T is proportional to the thermal climb velocity. The parameter ς represents the variance of the dislocation bias (defined below). Such a variance arises for the fact that the long-range stress field of dislocations contained in dipoles and dense tangles is significantly less that the stress field of isolated

dislocations. Estimates given by Wolfer, Ashkin, and Boltax [16] indicate that the bias of dislocations in dipoles is reduced by about a factor of two in comparison to the bias of an isolated dislocation.

Since a cold-worked dislocation structure is expected to contain most of the dislocations in dense tangles, the bias variance is expected to be larger than in an annealed dislocation structure. Assuming then a normal distribution for individual bias factors with a standard deviation of $\sqrt{\frac{2}{\pi}}\varsigma$, and an exponential increase of the bias variance with the dislocation density, the following form is chosen for the variance:

$$\varsigma = \frac{1}{\sqrt{2\pi}}[1 - e^{-L\rho}] \quad . \tag{12}$$

Here, the exponential term and $L = 1 \times 10^{-15}$ m^2 is selected such that the bias variance becomes negligible for dislocation densities less than 1×10^{15} m^{-2}. The impact of the bias variance is that individual dislocations can still climb in the absence of cavities, a fact borne out by the radiation-induced recovery of cold-worked materials prior to void swelling.

This recovery process is modeled by considering the climb of edge dislocations in a dipole. If the two dislocations converge onto the same glide plane, and if their mutual interaction can also overcome the critical resolved shear stress τ_o for glide, then it can be shown [15] that the rate of dislocation annihilation is given by

$$A\rho^2 = \frac{1}{12}h_{max}V_R + \frac{1}{6}HbV_T \ln\left[\frac{h_{max}}{b}\right] \tag{13}$$

where

$$h_{max} = \min\left[8\sqrt{\frac{3}{\pi\rho}}, \frac{l}{\ln[l/b]}\right] \tag{14}$$

is the largest dipole width. This width is either determined by the dislocation density ρ or or by the condition of overcoming the shear stress τ_o. This stress is assumed to be about equal to the critical stress for activating a Frank-Read source with a mesh length of l. The dislocation evolution is now determined by the rate equation

$$\frac{d\rho}{dt} = B\rho - A\rho^2 \, . \tag{15}$$

This equation resembles the empirical one proposed recently by Garner and Wolfer [14], and the above model provides a physical basis for it. It must be noted, however, that in contrast to the empirical evolution equation, the parameters A and B depend on the sink strengths, i.e. on the dislocation density itself. Equation (15) therefore requires numerical integration.

The bias variance and the mesh length l were determined by comparing the results of the present model with dislocation densities observed in irradiated type 316 stainless steel. The choice of L given above and $l = 4 \times 10^{-7}$ m gave satisfactory agreement, and Figure 2 shows the dislocation evolution for type 316 stainless steel. Using the same values for L and l, but material parameters for body centered cubic iron, the dislocation evolution for ferrite phase is predicted as illustrated in Figure 3.

Discussion and Results

The swelling model described above has been coded into a computer program known as WINGRA (WIsconsiN Growth RAte code). The flow diagram, Table 1, summarizes the method of determining swelling rate and swelling. It also illustrates how bias factors and sink strengths are continuously evaluated as the microstructure evolves. The results of the model are as follows.

1. Athermal processes (self-interstitial emission and loop punching) are not activated unless blistering type conditions are modeled for which the He/dpa ratio is about 1000.
2. Thermal vacancy exchange is not important until higher temperatures are reached. For austenitic stainless steels the temperature must exceed $600°C$. For ferrite phase the temperature must exceed $500°C$. The minimum temperature where thermal vacancy exchange becomes noticeable is determined by the vacancy migration energy. The values for this energy along with other parameters of interest can be seen in Table 2.
3. Bias driven growth is the most important growth mechanism for temperatures below 500 and $600°C$ for ferrite phase and austenitic stainless steels, respectively.

Two different steels (austenitic stainless steel and ferrite phase) were modeled for two different helium build-up rates (20 appm He/dpa and 0.6 appm He/dpa) with two different material starting conditions (cold-worked and annealed). The two Figures 4 and 5 show the results for swelling. An explanation of the results follows.

For 316 austenitic stainless steel a steady state swelling rate of between 0.7 %/dpa and 1.3 %/dpa is calculated for temperatures between $300^{o}C$ and $600^{o}C$. The variation in steady state swelling rates is due mainly to variations in sink strengths. The lower the temperature the higher the void number density; hence, the greater the difference between void and steady state dislocation sink strength. At higher temperatures the sink strengths are closer to being equal and a higher swelling rate is calculated.

For ferrite phase a steady state swelling rate of between 0.01 %/dpa and 0.3 %/dpa is calculated. Once again the difference in swelling rate can be attributed to variation in steady state sink strengths between voids and dislocations.

For both steels at 20 appm He/dpa, differences in early swelling rates for annealed versus cold-worked material at $300^{o}C$ can be attributed to the time evolution of the dislocation density. The annealed material takes longer to reach a steady state dislocation density than does cold-worked material. Therefore, a more slowly increasing swelling rate for $300^{o}C$ can be seen for the annealed material than for the cold-worked material. However, as stated previously the small dislocation loops have not been accounted for.

For both steels at 0.6 appm He/dpa an incubation-type period is observed at early times. This latent period is due to there not being sufficient helium pressure to force the cavities to grow to sufficient size for bias driven growth to dominate. However, once the cavity reaches a critical size for bias driven growth to become dominant, the voids grow according to rate theory calculations. This then explains the rapid changes in slope for swelling as a function of dose. The latent period of very slow void growth is due to the interplay of two factors. First, small vacancy clusters whether empty or filled with helium, possess a significant bias for preferential interstitial absorption due to the image interaction; this bias decreases,however,with increasing cavity radius. The small cavities are stabilized by the helium and growth requires, for some period, the continuing

capture of additional helium. As a result, the pressure in small cavities becomes very large which in turn enhances bias driven growth, and the pressure decreases rapidly as the radius increases. Figure 6 shows the net pressure $(p - 2\gamma/R)$ as a function of dose for the two helium production rates of 0.6 and 20 appm He/dpa. It is seen that the small cavities are extremely over-pressurized but with increasing dose rapidly convert to voids as already pointed out by Stoller and Odette [17]. Bias driven growth becomes dominant after $(p - 2\gamma/R)$ reaches its minimum. It is found that this conversion to a bias driven void occurs at a radius of about 1.2nm independent of the helium production rate.

The present void growth model for swelling needs several improvements before the swelling predictions can be compared with experiments. Most importantly, it is necessary to allow for time-dependent vacancy cluster formation in order to obtain a cavity size distribution. This will produce a more gradual transition in swelling from the transient period to the steady state period. A second modification will also be required to allow for the continued formation of small helium bubbles in the presence of already existing large voids whenever the helium production rate is high. The formation of a bimodal cavity distribution has been observed in HFIR irradiated type 316 stainless steels [18,19]. However, present models of cavity nucleation are not yet capable of predicting the number of cavities produced after a certain irradiation period. These data must be obtained from experiments and treated as input to theoretical void growth models.

Acknowledgments

This work was supported in part by the Electric Power Research Institute under contract RP1597-2 and in part by the United States Department of Energy under contract DE-AC02-82ER50282 with the University of Wisconsin.

References

[1.] Garner, F. A., *J. Nucl. Mater.*, to be published.

[2.] Gelles, D. J., *J. Nucl. Mater.*, to be published.

[3.] Trinkaus, H. and Wolfer, W. G., *J. Nucl. Mater.*, to be published.

[4.] Wolfer, W. G., Glasgow, B. B., Wehner, M. F., and Trinkaus, H., *J. Nucl. Mater.*, to be published.

[5.] Wolfer, W. G., "Effects of Radiation of Materials", *ASTM STP 725* (1980) 201.

[6.] Carnahan, N. F. and Starling, K. E., *J. Chem. Phys.* **51** (1969) 635.

[7.] Young, D. A., McMahon, A. K., and Ross, M., *Phys. Review* **B24** (1981) 5119.

[8.] Hansen, J. P. and Pollock, E. L., *Phys. Review* **A5** (1972) 2651.

[9.] Glasgow, B. B. and Wolfer, W. G., *J. Nucl. Mater.*, to be published.

[10.] Trinkaus, H., *Rad. Effects* **78** (1983) 189.

[11.] Greenwood, G. W., Forman, A. J. E., and Rimmer, D. E., *J. Nucl. Mater.* **4** (1959) 305.

[12.] Harkness, S. D. and Li, C. Y., "Proceedings of the International Conference on Radiation-Induced Voids in Metals", J. W. Corbett and L. C. Ianniello, Eds., (1971) 798.

[13.] Sniegowski, J. J. and Wolfer, W. G., "Proceedings of the Topical Conference on Ferritic Alloys for Use in Nuclear Energy Technologies", June 1983, to be published.

[14.] Garner, F. A. and Wolfer, W. G., "Effects of Radiation on Materials", *ASTM STP 782* (1982) 1073.

[15.] Wolfer, W. G. and Glasgow, B. B., "A Rate Theory Model for the Evolution of Network Dislocations in Irradiated Metals", to be published.

[16.] Wolfer, W. G., Ashkin, M., and Boltax, A., "Properties of Reactor Structural Alloys After Neutron of Particle Irradiation", *ASTM STP 570* (1975) 233.

[17.] Stoller, R. E. and Odette, G. R., "A Model Based Fission-Fusion Correlation of Cavity Swelling in Stainless Steel", *J. Nucl. Mater.* **104** (1981) 1361.

[18.] Maziasz, P. J., *J. Nucl. Mater.* **108** (1982) 359.

[19.] Maziasz, P. J., "Comparison of Swelling and Cavity Microstructure Development for Type 316 Stainless Steel Irradiated in EBR-II and HFIR", *J. Nucl. Mater.*, to be published.

Table 1

1. Initialize the problem; set constraints: material parameters, dose rate, helium buildup rate, initial dislocation density.

2. For a given temperature determine the dislocation bias factors $Z^d_{i,v}$, set the temperature dependent parameters.

3. Given a swelling, helium density, and temperature determine compressibility factor z and pressure in the cavity.

4. Determine void bias factors $Z^o_{i,v}$ and sink strengths $S_{o,d}$. Find sink averaged bias factors and vacancy concentration, $\bar{Z}_{i,v}$ and $\bar{C}_v$.

5. Calculate swelling rate and dislocation density rate of change. Find a suitable time step and increment swelling and dislocation density. Go to step 3 as necessary.

Table 2

	316 SS	ferrite
lattice parameter (m)	3.639×10^{-10}	2.8664×10^{-10}
vacancy relaxation volume (Ω)	-0.2	-0.5
interstitial relaxation volume (Ω)	1.5	0.85
vacancy formation energy (J)	2.88×10^{-19}	2.464×10^{-19}
interstitial formation energy (J)	9.6×10^{-19}	9.6×10^{-19}
vacancy migration energy (J)	1.92×10^{-19}	2.016×10^{-19}
interstitial migration energy (J)	2.4×10^{-20}	3.2×10^{-20}
vacancy diffusion constant (m^2/sec)	1.29×10^{-6}	4.463×10^{-5}
dpa rate (dpa/sec)	1.0×10^{-6}	1.0×10^{-6}
cascade efficiency	0.1	0.1

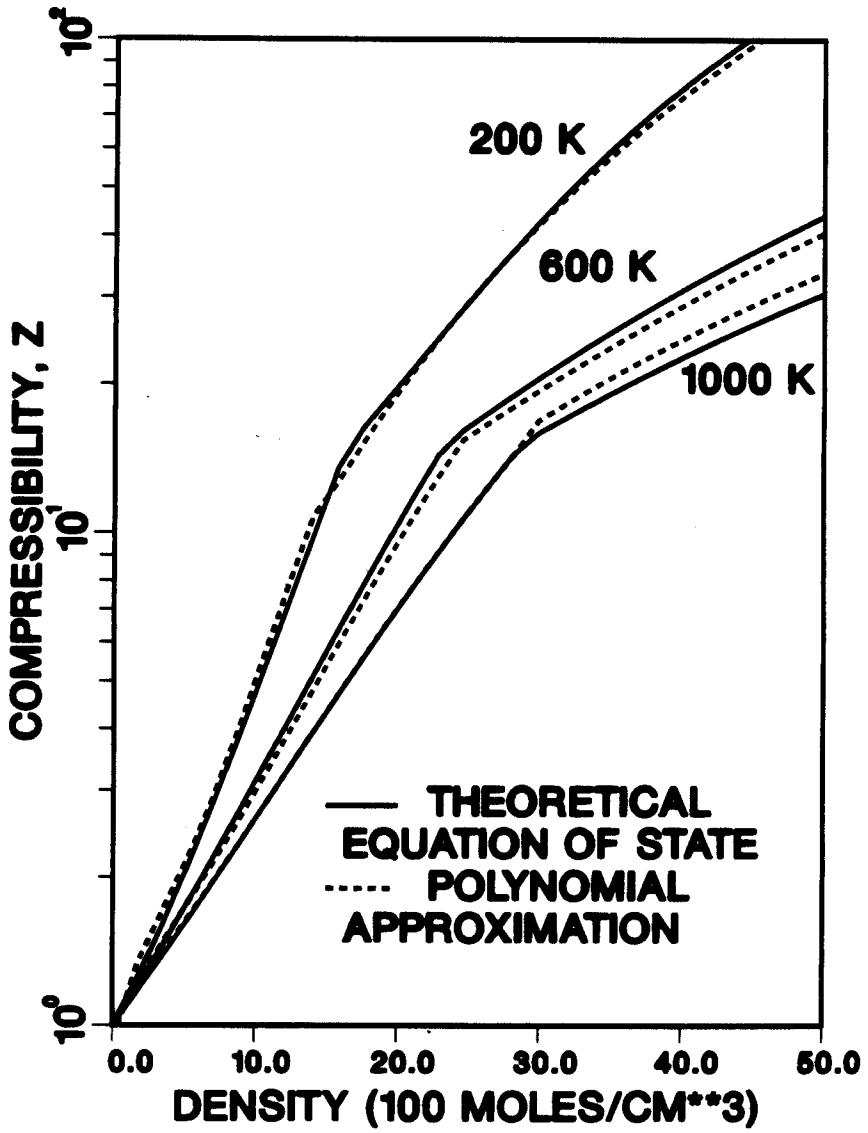

Figure 1. Compressibility factor versus helium density for various temperatures. The fitted polynomial equation of state is compared to the detailed theoretical equation of state.

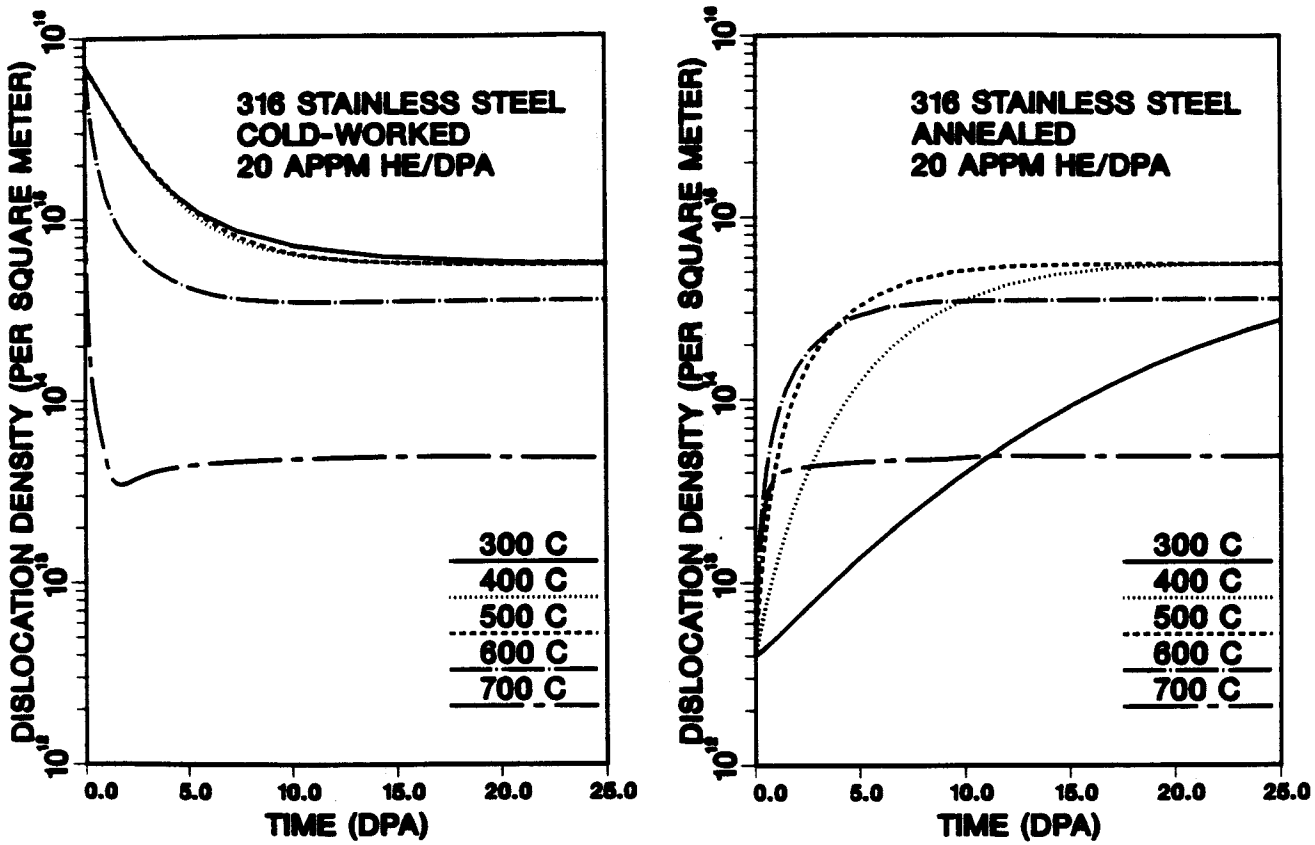

Figure 2. Dislocation density versus dpa for various temperatures. Cold-worked and annealed 316 austenitic stainless steel starting conditions are modeled. The results for 0.6 appm He/dpa show similar results except the steady state density for $700^{o}C$ is approximately half as high.

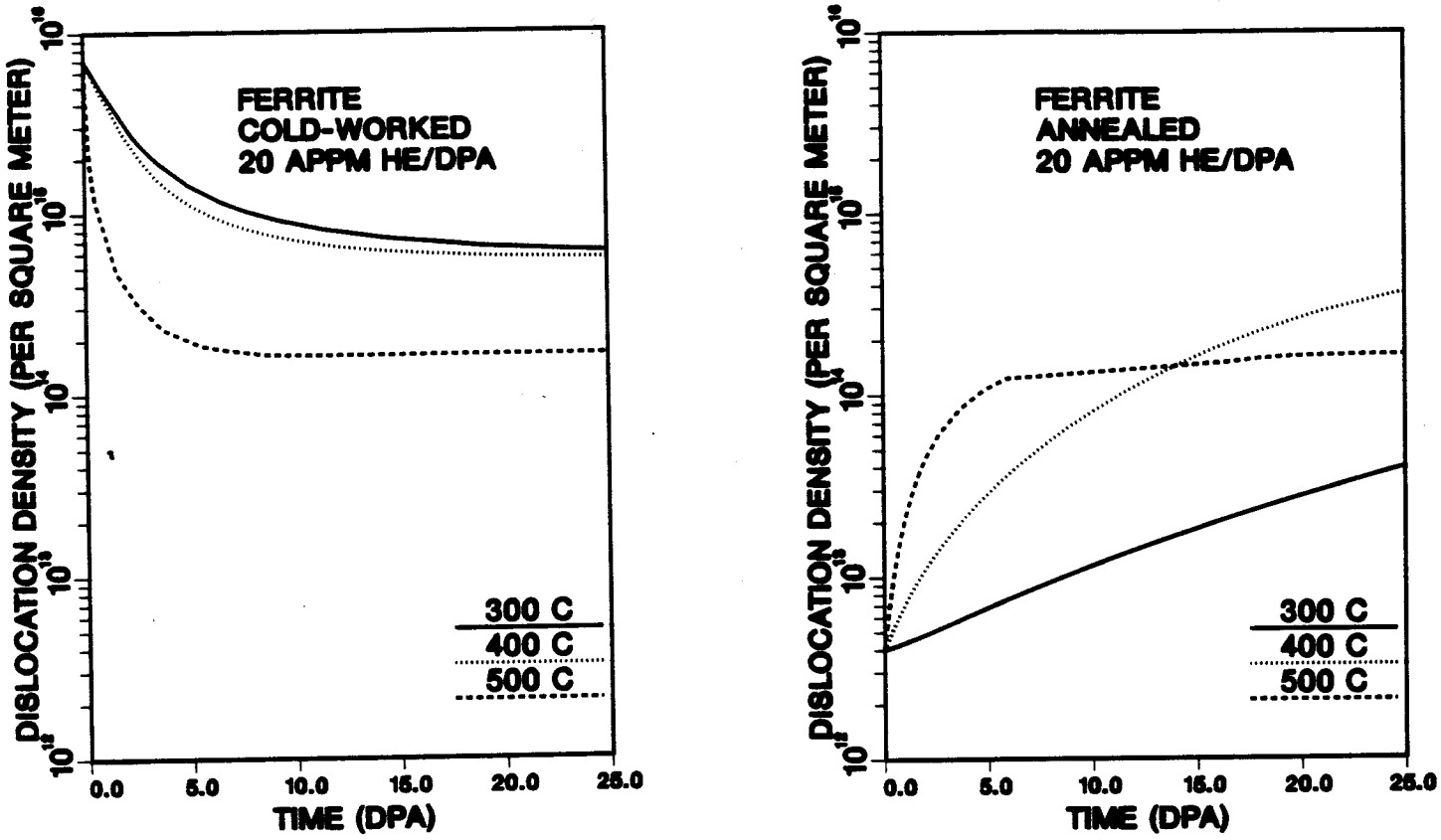

Figure 3. Dislocation density versus dpa for various temperatures. Cold-worked and annealed ferrite phase starting conditions are modeled. The results for 0.6 appm He/dpa show similar results.

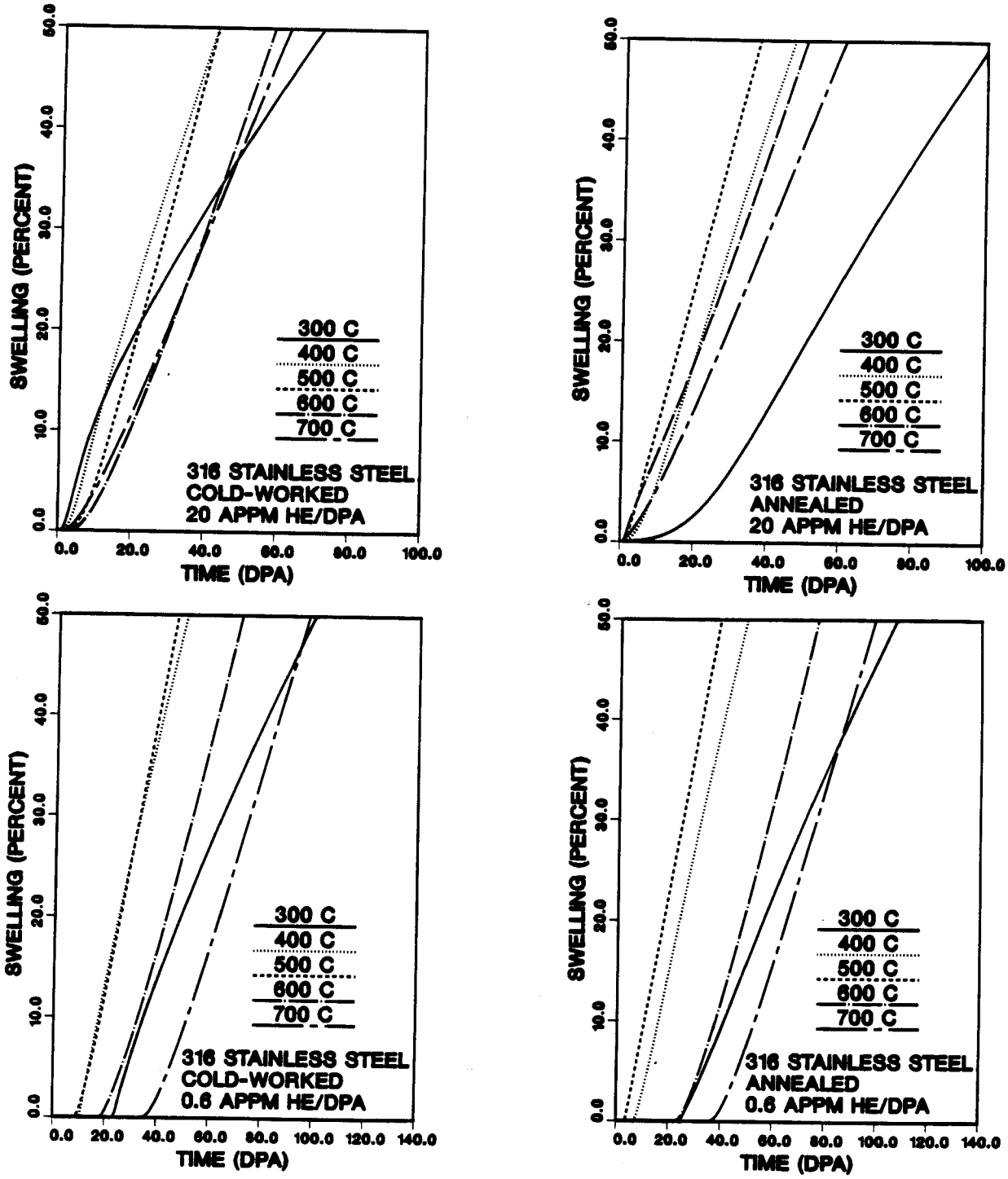

Figure 4. Swelling versus dpa for various temperatures. Cold-worked and annealed 316 austenitic stainless steel starting conditions are modeled for different He/dpa ratios.

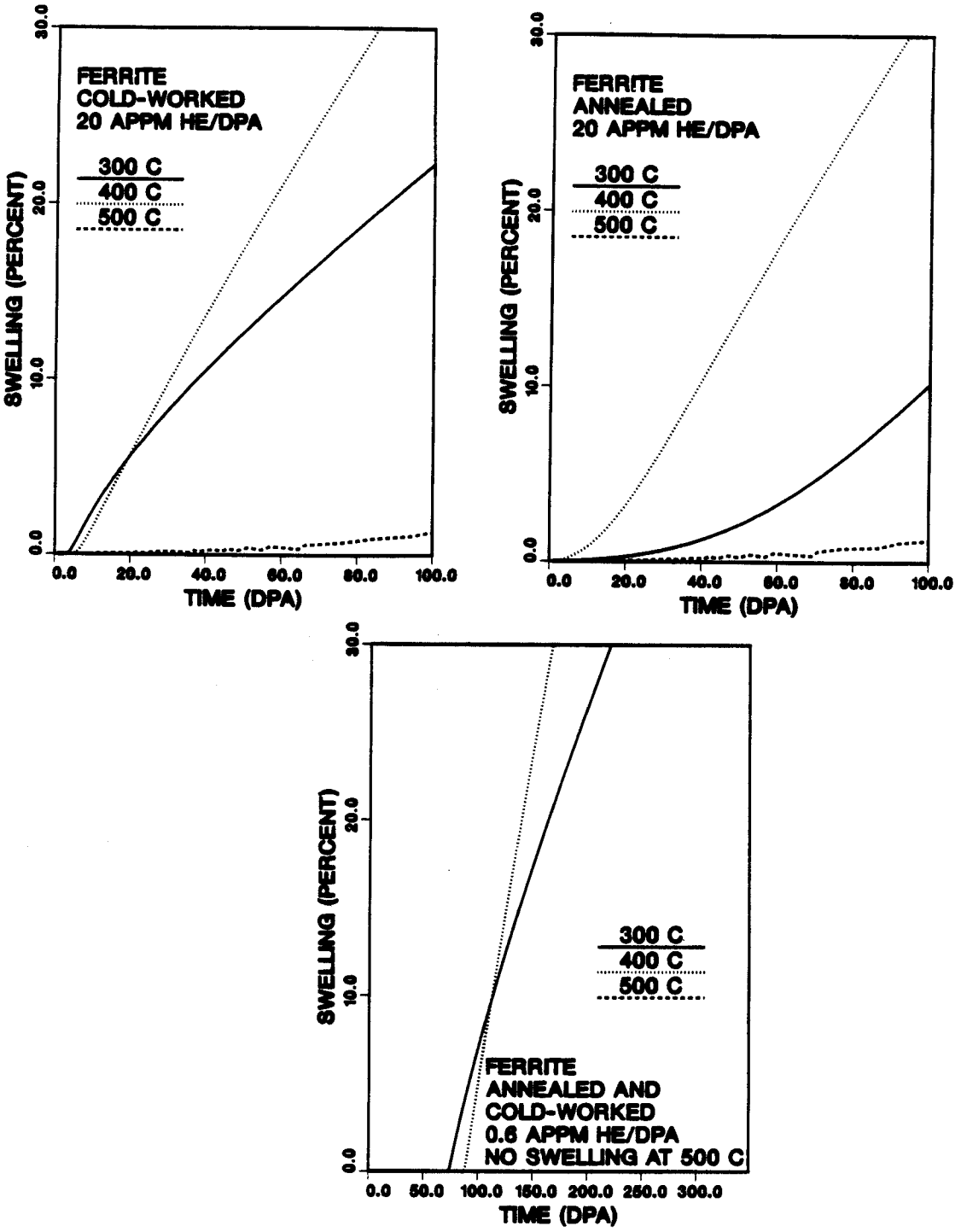

Figure 5. Swelling versus dpa for various temperatures. Cold-worked and annealed ferrite phase starting conditions are modeled for different He/dpa ratios. Swelling rates for the 0.6 appm He/dpa case are the same for both cold-worked and annealed because the onset of swelling occurs after steady state dislocation density is reached.

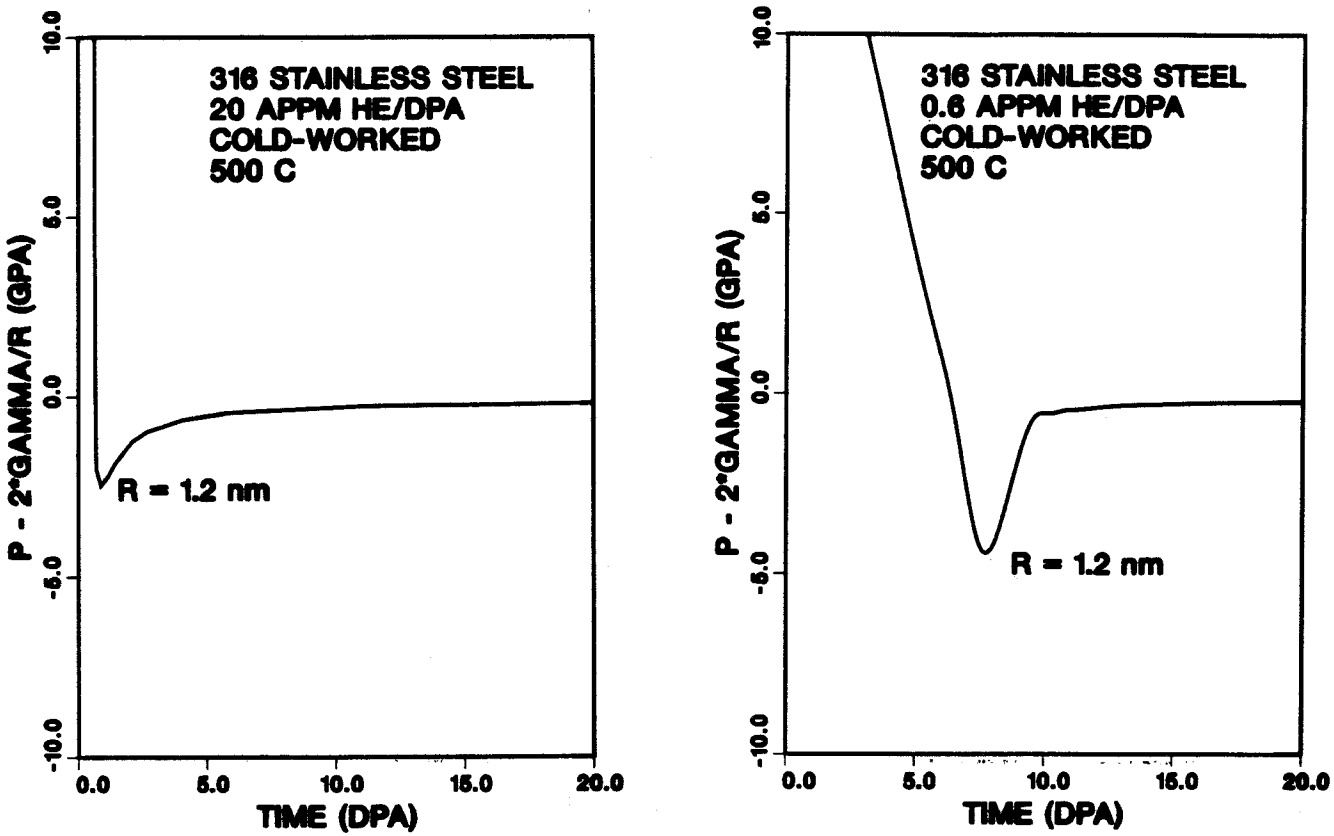

Figure 6. Net pressure versus dpa for two different He/dpa rates. In both cases the minimum occurs at approximately 1.2nm.